Effects of loading rate on the dynamic behavior of polypropylene fiber reinforced concrete: an experimental investigation

Wang Youshi[1], Liu Zhongzhong[2], Wu Guojun[2], Zhao Baofeng[3], Wang Fengxi[3,4], Lin Chao[1,*], Qiu Xin[5], Wang Jianjun[3], Yu Jiawu[3], Gao Zhipeng[1]

1. Yichun University, Yichun 336000, Jiangxi, China
2. China University of Mining and Technology, Xuzhou 221116, Jiangsu, China
3.China Railway Tunnel Group Second Division Co., Ltd., Langfang 065201, Hebei, China
4.China Railway No.16 Bureau Group No.5 Engineering Co., Ltd., Tangshan 064099, Hebei, China
5. Institute of Rock and Soil Mechanics, Chinese Academy of Sciences, Wuhan 430071, Hubei, China

Abstract: Cyclic dynamic loading accelerates the propagation of initial cracks in concrete, leading to damage and failure. To investigate the effect of polypropylene fiber content on the dynamic compressive and tensile properties of concrete, a self-developed rock-concrete mechanical testing system was employed to examine responses under varying loading rates (10^{-5}-10^{-2}/s). The study evaluated elastic modulus, peak strain, toughness index, and related indicators. Results show that both compressive and tensile strengths of fiber-reinforced concrete increase with loading rate and exceed those of plain concrete. Specifically, at a loading rate of 10^{-2}/s, the compressive strength and splitting tensile strength of plain concrete are 61.51 MPa and 1.43 MPa, respectively, while those of fiber-reinforced concrete reach 67.96 MPa and 2.6 MPa. Fiber addition improves peak strain, toughness, and failure mode, significantly enhancing resistance to damage and deformation. This study provides a theoretical basis for the engineering application of fiber-reinforced concrete under dynamic loading and paves the way for future research on related dynamic constitutive models and numerical simulations.

Keywords: Polypropylene fiber content; Dynamic compressive property; elastic modulus; Toughness index; Loading rate.

1 Introduction

Concrete, as the most widely used and abundant construction material today, holds an irreplaceable role in various fields of civil engineering[1-2]. Nevertheless, it suffers from inherent shortcomings such as low tensile strength, poor crack resistance, and limited toughness. To address these deficiencies, researchers worldwide have been actively exploring strategies to enhance concrete performance, including the development of new additives to broaden its application scope and adaptability[3-4]. Among these innovations, ultra-high-performance concrete (UHPC), a novel cement-based composite, has emerged as a key research direction[5]. Owing to its dense micro-structure and outstanding strength, ductility, and durability, UHPC can significantly extend the service life of concrete structures. At present, incorporating polypropylene fibers is a common method for strengthening concrete and improving its crack resistance[6-7]. These fibers not only inhibit crack initiation and propagation within the concrete matrix but also enhance its tensile strength and toughness[8].

Polypropylene fiber reinforced concrete (PFRC) has emerged as a high-performance building material widely used in various civil engineering structures, such as blast-resistant facades, impact-resistant pavements, and seismic-resistant elements[9]. Its popularity stems from the remarkable enhancement in toughness, crack resistance, and energy absorption capacity imparted by the incorporation of polypropylene fibers, which effectively bridge micro-cracks and delay their propagation under mechanical stress[10-12].

Extensive experimental investigations have been conducted to characterize the mechanical properties of PFRC. Numerous studies[13-16] have firmly established that the addition of polypropylene fibers significantly improves the quasi-static properties of concrete, including its flexural strength, fracture energy, and post-cracking ductility. Research has also delved into the effects of fiber parameters, such as length, diameter, aspect ratio, and volumetric dosage, on these static mechanical performances, providing valuable guidelines for material design[17-18].

However, many of the critical applications for PFRC involve dynamic loading scenarios, such as explosions, impacts, and seismic events. The mechanical behavior of concrete is highly sensitive to strain rate, a phenomenon known as the dynamic increase factor (DIF). Despite the wealth of research on its static performance, a significant gap remains in the systematic understanding of the dynamic behavior of PFRC, particularly concerning the effect of loading rate. While a limited number of studies[19-20] have explored the dynamic compressive or tensile strength of fiber-reinforced concrete using split Hopkinson pressure bar (SHPB) apparatus or servo-hydraulic systems, the existing body of work exhibits two primary limitations:(1) Many studies compare only a limited number of discrete strain rates (e.g., static vs. a single high rate), failing to provide a continuous and comprehensive picture of how mechanical properties evolve across a wide spectrum of loading rates[21-22]; (2) The synergistic effects between polypropylene fibers and the rate-sensitive cementitious matrix are not fully elucidated. It remains unclear how the fiber-matrix interface debonding, fiber pull-out mechanism, and crack-bridging efficiency are influenced by varying loading rates.

Therefore, this paper presents a detailed experimental investigation into the effects of loading rate on the dynamic mechanical properties of polypropylene fiber reinforced concrete to address these research deficiencies. A series of tests are conducted over a wide range of precisely controlled loading rates using the RMT-201 rock and concrete testing system. The dynamic compressive strength and deformation characteristics are meticulously measured and analyzed. The findings of this study aim to bridge the current knowledge gap, providing crucial data and insights for the more rational design and application of PPRC in structures subjected to dynamic loads.

The main contents of this study is as follows. Section 2 introduces the experimental scheme of polypropylene fiber reinforced concrete under compression loading. Some analyses of mechanical properties of fiber concrete are discussed in Section 3. Following this, Section 4 presents the analysis of mechanical properties of concrete under the tensile loading. Finally, Section 5 summarizes some significant finding of the study.

2 Experimental scheme of polypropylene fiber reinforced concrete

2.1 Testing equipment

Dynamic compression and tension tests on polypropylene fiber reinforced concrete were conducted using the RMT-201 rock and concrete testing system (Wuhan Institute of Rock and Soil Mechanics) as shown in Fig.1. Standard and fiber-reinforced concrete specimens (fiber content: 1.2 kg/m^3) were prepared. Tests were performed across strain rates from quasi-static to dynamic loading (10^{-5}, 10^{-4}, 10^{-3}, and $10^{-2}s^{-1}$).

The system integrates loading, control, and calibration modules, with a maximum load capacity of 3000kN and a loading rate up to 30mm/s. It also allows automatic switching between force- and displacement-control modes for matched dynamic testing.

(a) Compression test (b) Tensile test

Fig. 1 Test setup for loading concrete specimens.

2.2 Polypropylene concrete materials and mix proportions

The concrete was designed with a strength grade of C50 and a water–cement ratio of 0.58. The mix proportion of the polypropylene fiber reinforced concrete was cement : mineral powder : fly ash : water : medium sand : crushed stone = 1 : 0.33 : 0.33 : 0.58 : 2.84 : 3.77. Steel fiber contents were set at 0 and 1.2 kg/m^3. A polycarboxylate superplasticizer (1.9%) was added to improve workability. The detailed parameters of the polypropylene fibers used in the tests are listed in Table 1, reflecting the actual project application.

Table 1 Main physical and mechanical parameters of fibers

Parameter	Unit	Value
Density	kg/m^3	0.91
Length	mm	9
Diameter	μm	20
Tensile strength	MPa	570
Elasticity modulus	GPa	7.2
Breaking elongation	%	35
fiber content	kg/m^3	1.2

2.3 Preparation of test blocks

Concrete specimens were prepared using raw materials from the Qingdao Metro construction site. Dynamic uniaxial compression and tensile tests were performed on specimens of different shapes and sizes. Cubic specimens (150 × 150 × 300 mm) were used for compression tests (see Fig. 2a and Table 2), and cylindrical specimens (50 × 30mm) for tensile tests (see Fig. 2b and Table 3). Tests were conducted at increasing strain rates (10^{-5}, 10^{-4}, 10^{-3}, and 10^{-2} s^{-1}) to investigate the dynamic mechanical properties of the specimens. The mixed fiber concrete was cast into standard plastic molds in three layers, each vibrated for 2 min until fully compacted. The molds were then covered with cling film to prevent water evaporation. After 24 h, the specimens were demoulded and transferred to a standard curing room (20 ± 2 °C, >95% RH) for water curing.

(a)Compression loading test block (b)Tensile loading test block

Fig. 2 Concrete loading test block.

Table 2 Preparation parameters of dynamic compression test blocks

No	Strength grade	number	Fiber content(kg/m^3)	Size		
				Length(mm)	Width(mm)	Height(mm)
C50S1.2	C50	3	1.2	150	150	300
C50S0	C50	3	0	150	150	300

Table 3 Preparation parameters of dynamic tensile test blocks

No	Strength grade	number	Fiber content(kg/m^3)	Size	
				Diameter(mm)	Height(mm)
C50S1.2	C50	3	1.2	50	30
C50S0	C50	3	0	50	30

3 Analysis of mechanical properties of fiber Concrete under Compression loading

3.1 Compressive strength analysis

Fig.3 illustrates the influence of the loading rate on the compression strength σ_c and the growth rate η of σ_c. It should be noted that the reported compressive strength represents the average of three specimens from the same group. η denotes the increase in compressive strength of fiber-reinforced concrete relative to the reference concrete under the same loading rate. From Fig. 3, the following conclusions can be drawn: (1) At a quasi-static loading rate of $10^{-5}s^{-1}$, polypropylene fibers have little effect on compressive strength (55.15MPa for fiber reinforced concrete vs. 55.7MPa for reference concrete). However, as the loading rate increases (10^{-4}-$10^{-2}s^{-1}$), the fiber-reinforced specimens exhibit a pronounced strength gain, with the improvement rising from -1.1% to 10.5%. At 10^{-2} s^{-1}, the compressive strength reaches 67.96MPa compared with 61.51MPa for reference concrete; (2) Both fiber-reinforced and reference concrete show the same general trend: compressive strength increases significantly with loading rate; (3)Under quasi-static conditions (i.e., the loading rate is 10^5s^{-1}), fibers had little influence on compressive strength: 55.15MPa for fiber-reinforced concrete versus 55.7MPa for the reference concrete. However, under dynamic loading (10^{-4}-$10^{-2}s^{-1}$), the fiber-reinforced specimens exhibited markedly higher strength than the reference specimens, with the improvement increasing with loading rate. At $10^{-2}s^{-1}$, the compressive strength reached 67.96MPa for fiber-reinforced concrete, compared with 61.51MPa for the reference concrete.

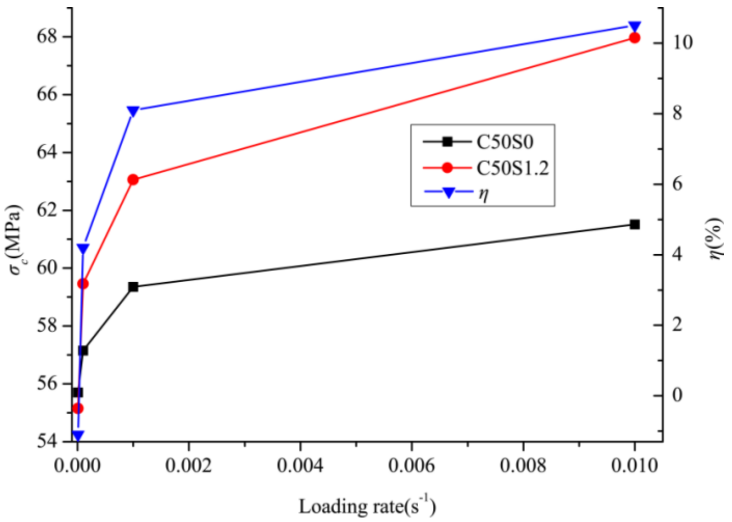

Fig. 3 Influence of the loading rate on σ_c and η .

To characterize the dynamic strength of fiber-reinforced concrete and the influence of loading rate, the dynamic increase factor (DIF) is commonly used to relate strain rate to compressive strength. Various empirical models have been proposed to describe the dynamic strength of concrete under different loading rates, including exponential, logarithmic, and CEB-based formulations. Among them, logarithmic expressions are most commonly used owing to their simplicity and accuracy. Accordingly, a logarithmic function is adopted in this study, as given in Eq.(1).

$$\frac{F_j}{F_d} = A + B\lg\left(\frac{\varepsilon'}{\varepsilon'_s}\right) \tag{1}$$

Where F_j is the quasi-static compressive strength, F_d is the dynamic compressive strength, ε' is the dynamic loading strain rate, ε'_s is the strain rate under quasi-static loading, and A and B are the fitting parameters, respectively.

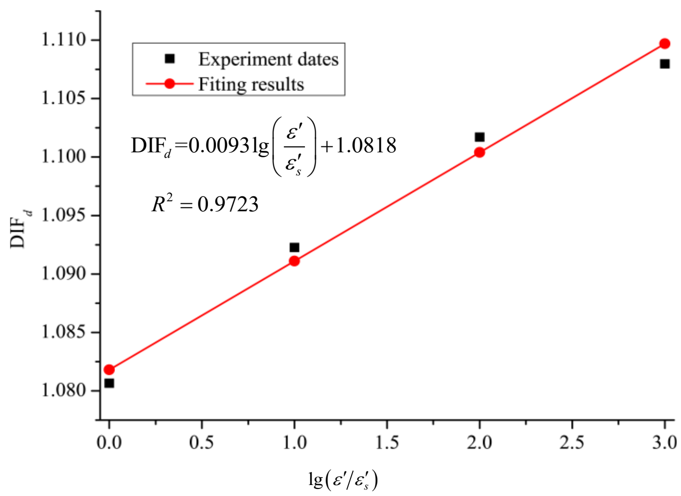

Fig. 4 Calculated curve of DIF$_d$

As shown in Fig. 4, Eq. (1) accurately captures the relationship between DIF$_d$ and $\lg\left(\frac{\varepsilon'}{\varepsilon'_s}\right)$, with R^2 =

0.9723. Moreover, DIF_d increases linearly with $\lg\left(\frac{\varepsilon'}{\varepsilon_s'}\right)$. Specifically, as $\lg\left(\frac{\varepsilon'}{\varepsilon_s'}\right)$ rises from 0 to 3, DIF_d increases from 1.0818 to 1.1097, corresponding to a gain of about 25.8%.

3.2 Evaluation of the compression loading characteristics

Under uniaxial compression, the stress–strain curves of concrete specimens with varying fiber contents are shown in Fig.5. The results indicate that: (1) In the peak region, both fiber-reinforced and reference concrete exhibit higher compressive strength at higher loading rates, with the peak stress increasing accordingly. Before the peak, the curves are similar, showing rapid stress growth, whereas after the peak, fiber-reinforced concrete demonstrates superior performance, with a gentler stress decline and a transition from quasi-brittle to elastoplastic behavior with high ductility; (2) Fiber incorporation enhances mechanical properties by increasing the ultimate compressive strength in the pre-peak stage and improving deformation resistance and ductility in the post-peak stage. The gentler post-peak curve confirms the positive effect of fibers on matrix ductility.

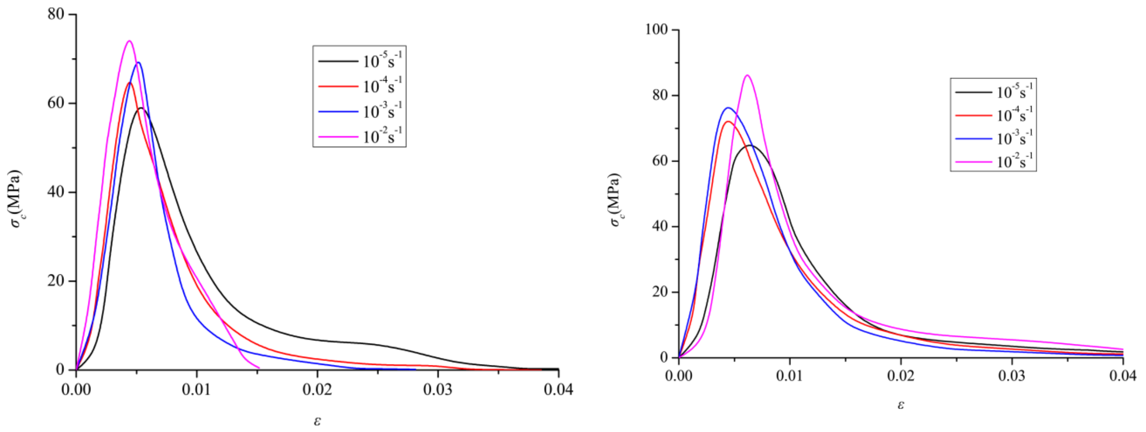

(a)C50S0 test block (b) C50S1.2 test block

Fig. 5 Uniaxial compression stress-strain curves of specimens at different strain rates

3.3 Mechanical properties of uniaxial compression loading

The measured elastic modulus E of fiber-reinforced and control concrete specimens is shown in Fig.6. Under the same strain rate, both exhibit nearly identical values. At a loading rate of 10^{-5}/s, the elastic modulus is 34.1 GPa for the control and 34.2 GPa for the fiber concrete, while at 10^{-2}/s, the values are 34.2 GPa and 34.3 GPa, respectively. These results indicate that loading rate has little influence on the elastic modulus, confirming that this parameter is essentially strain-rate insensitive.

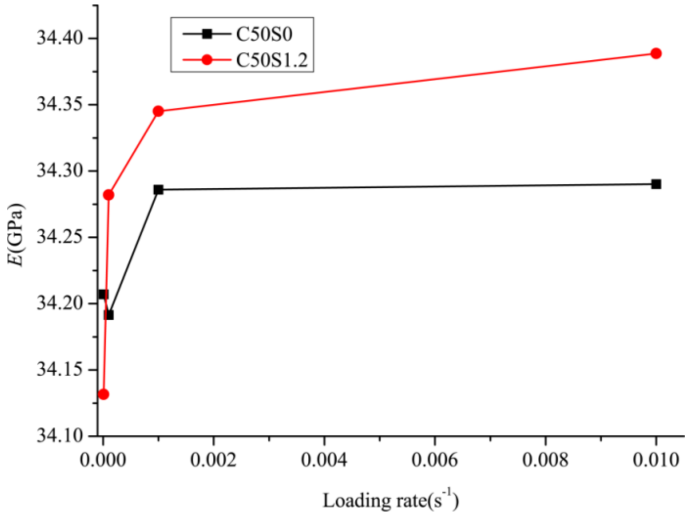

Fig. 6 Influence of loading rate on *E*

Fig.7 illustrates the effect of loading rate on peak strain ε_p . At the same loading rate, fiber-reinforced concrete exhibits higher peak strain than the reference concrete, indicating enhanced deformation resistance due to fiber addition. For example, at 10^{-5}/s, the peak strain is 3.45×10^{-3} for fiber-reinforced concrete and 3.1×10^{-3} for the reference specimen, while at 10^{-2}/s the values are 2.95×10^{-3} and 2.7×10^{-3}, respectively. Moreover, peak strain decreases as loading rate increases.

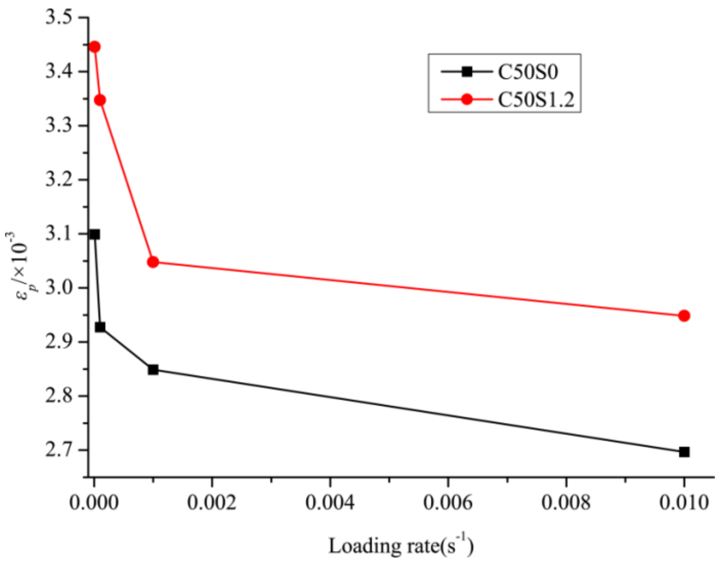

Fig. 7 Influence of loading rate on ε_p

Previous studies have reported that in uniaxial compression tests of fiber-reinforced concrete, the toughness index ξ decreases with increasing fiber content. The toughness index ξ of fiber-reinforced concrete is defined as

$$\xi = \frac{S_\Delta}{\delta} \tag{2}$$

Where ξ is the consumed energy within the *OACD* region of the stress-strain curve of the concrete material, and δ represents the elastic potential energy consumed by the concrete material. The area *OAB* of the stress-strain curve corresponding to 85% of the ultimate load is taken, as shown in Fig.8.

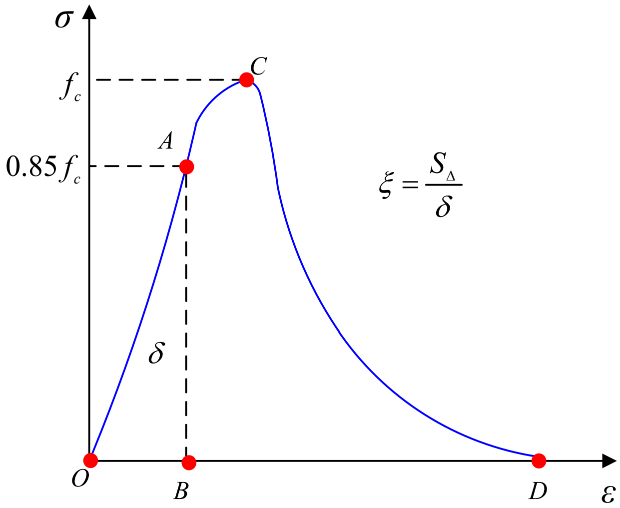

Fig. 8 Schematic diagram of the toughness index of fiber-reinforced concrete

Fig.9 shows the toughness index ξ of concrete with different fiber contents. Under identical loading conditions, fiber-reinforced specimens exhibit higher ξ than reference concrete. For example, at a loading rate of 10^{-5}/s, ξ of fiber-reinforced concrete is 7.47 compared to 6.41 for the benchmark concrete, while at 10^{-2}/s the values are 5.73 and 3.62, respectively. Overall, ξ decreases with increasing loading rate.

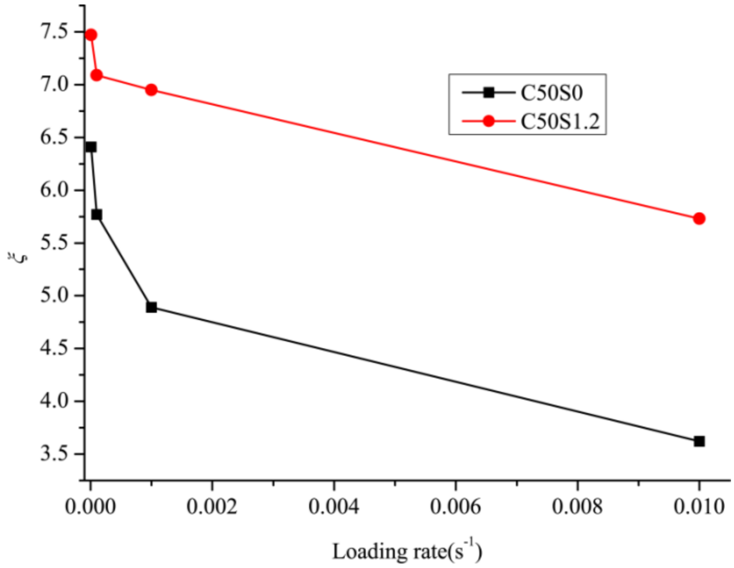

Fig. 9 Influence of loading rate on ξ

Fig.10 shows the influence of fiber content on the post-fracture morphology of concrete. As can be seen from the figure, there are significant differences in the post-fracture morphologies of the fiber concrete and the control concrete specimens. Adding fibers can effectively improve the brittle failure characteristics of the control concrete. When the control concrete fails, there is an instantaneous brittle collapse phenomenon, and the specimen breaks into a loose state with almost no residual strength. The fiber concrete specimen still has some residual strength after the peak. The fibers evenly distributed within the specimen can still bear part of the tension connection function. Due to the bridging effect of the fibers, the specimen can still maintain a relatively complete shape, and the residual strength remains at 2-4MPa, avoiding the brittle failure phenomenon of sudden collapse of the fiber concrete specimen after fracture.

(a) C50S0 (b) C50S1.2

Fig. 10 Failure morphology of the test block

4 Analysis of mechanical properties of fiber concrete under tensile loading

Fig.11 presents the measured tensile strength of fiber-reinforced and benchmark concretes. As shown, the tensile strength of both materials increases with loading rate, and the incorporation of fibers markedly enhances concrete strength. Specifically, at a loading rate of 10^{-5} s^{-1}, the splitting tensile strength of the fiber-reinforced specimen reaches 1.84 MPa, compared with only 1.25 MPa for the benchmark specimen. When the loading rate increases to $10^{-2}s^{-1}$, the measured values rise to 2.60 MPa and 1.43 MPa, respectively. Calculations indicate that the tensile strength of fiber-reinforced concrete is 46% higher than that of benchmark concrete. Moreover, although the relative strength advantage of fiber-reinforced concrete increases with loading rate, the rate of improvement gradually diminishes.

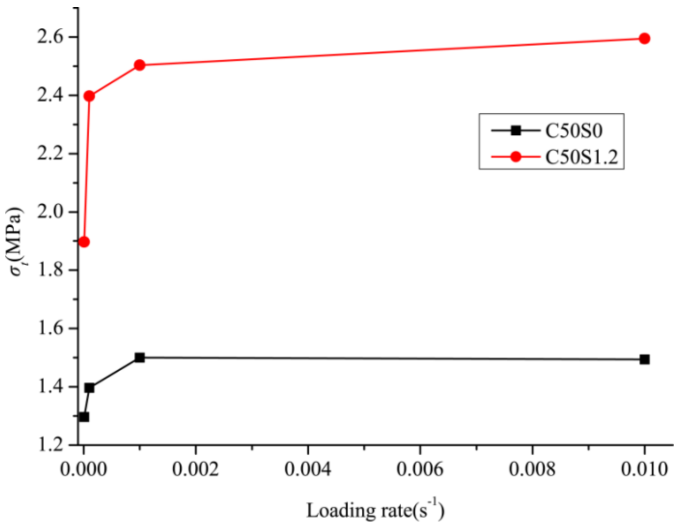

Fig. 11 Influence of loading rate on σ_t

This phenomenon can be attributed to the following: at low loading rates (10^{-5} s^{-1} and 10^{-4} s^{-1}), the fiber-bridging effect is more pronounced, and the tensile capacity primarily depends on the bridging resistance of fibers in combination with the tensile strength of the cementitious matrix. At higher loading rates (10^{-3} s^{-1}), however, coarse aggregates are rapidly sheared and crushed, leading to a reduced rate of strength gain. Consequently, under low strain rates, the fiber-bridging mechanism dominates, whereas with increasing strain rate, its effectiveness diminishes, and the failure mode transitions from tensile failure of the cementitious matrix to rapid shear failure of the coarse aggregates.

Fig.12 illustrates the effect of fibers on σ_t - ε response of concrete cores under tensile loading. The results demonstrate a pronounced strain-rate effect on the splitting tensile strength, namely, higher strain rates correspond to higher strengths. The incorporation of fibers markedly enhances the resistance of concrete to tensile failure. At a loading rate of 10^{-5} s^{-1}, the peak axial strain of the reference specimen is 8~10×10^{-3} whereas that of the fiber-reinforced specimen increases to 14~16×10^{-3}. After reaching the peak, the tensile strength of concrete decreases rapidly. At lower strain rates, the stress–strain curve descends gradually due to the adhesion of the cementitious matrix, while at higher strain rates it drops abruptly, with the peak axial strain reduced to 5×10^{-3} at the loading rate of $10^{-2}s^{-1}$.

These findings indicate that the reference concrete exhibits brittle splitting failure, whereas the post-peak mechanical response is significantly improved by fiber reinforcement. When the loading rate increases from $10^{-5}s^{-1}$ to 10^{-2} s^{-1}, the peak axial strain of the fiber-reinforced specimens decreases moderately, from 13×10^{-3} to 10×10^{-3}. After splitting failure, the tensile strength still declines, but the fibers provide bridging resistance that continues to bear load and restrain deformation, resulting in a gentler post-peak descending branch. Even at high loading rates, the stress-strain curve does not exhibit an abrupt vertical drop, highlighting the improved ductility of fiber-reinforced concrete.

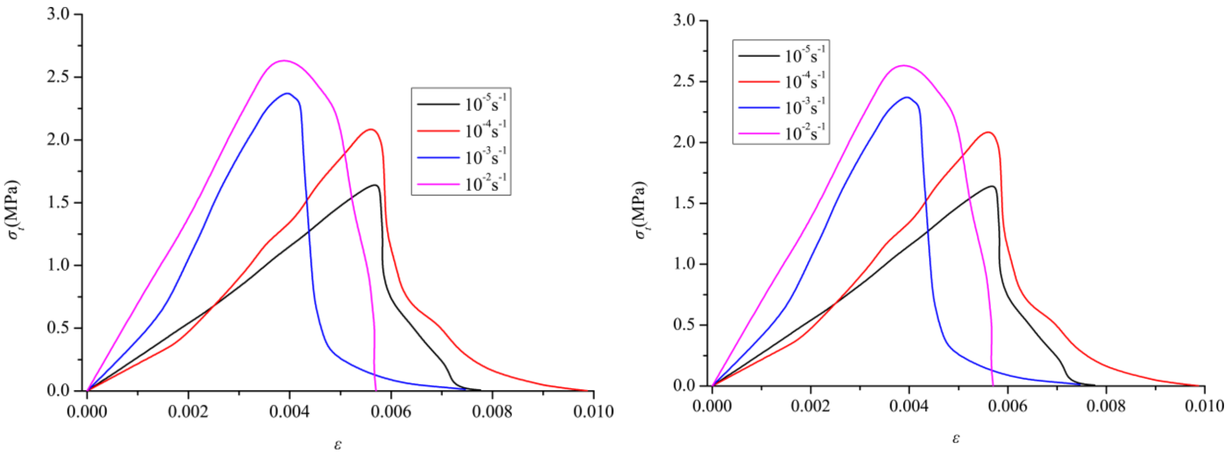

(a) C50S0 test block (b) C50S1.2 test block

Fig. 12 Tensile stress-strain curves of test blocks at different loading rates

5 Conclusion

This study investigated the dynamic mechanical behavior of polypropylene fiber-reinforced concrete, focusing on its compressive and tensile properties under varying loading rates. The main conclusions are as follows:

(1) Both the compressive and splitting tensile strengths of fiber-reinforced concrete exhibit a significant loading-rate strengthening effect. At a loading rate of 10^{-2} s^{-1}, the compressive and splitting tensile strengths of the fiber-reinforced specimens reach 67.96 MPa and 2.60 MPa, respectively, which are markedly higher than those of the reference concrete (61.51 MPa and 1.43 MPa), highlighting the pronounced enhancement of dynamic strength imparted by fiber incorporation.

(2) Compared with the reference concrete, the fiber-reinforced concrete demonstrates noticeably

higher peak strain and improved toughness indices, leading to superior overall mechanical performance. This indicates that the addition of fibers effectively enhances the deformation capacity and energy dissipation characteristics of the material.

(3) Compared with the reference concrete, the fiber-reinforced concrete demonstrates noticeably higher peak strain and improved toughness indices, leading to superior overall mechanical performance. This indicates that the addition of fibers effectively enhances the deformation capacity and energy dissipation characteristics of the material.

Acknowledgments

The authors acknowledge the financial support of the China Jiangxi Natural Science Foundation General Project (20232BAB204074).

References

[1] Tran V, Dang V, Ho L. Evaluating compressive strength of concrete made with recycled concrete aggregates using machine learning approach[J]. Construction and Building Materials, 2022, 323: 126578.

[2] Zhang C, Nerella V, Krishna A, et al. Mix design concepts for 3D printable concrete: A review[J]. Cement and Concrete Composites, 2021, 122: 104155.

[3] Alqarni A, Abbas H, Al-Shwikh K, et al. Treatment of recycled concrete aggregate to enhance concrete performance[J]. Construction and Building Materials, 2021, 307: 124960.

[4] Panghal H, Kumar A. Enhancing concrete performance: Surface modification of recycled coarse aggregates for sustainable construction[J]. Construction and Building Materials, 2024, 411: 134432.

[5] Bahmani H, Mostofinejad D. Microstructure of ultra-high-performance concrete (UHPC)–a review study[J]. Journal of Building Engineering, 2022, 50: 104118.

[6] Lakshmi A, Pandit P, Bhagwat Y, et al. A review on efficiency of polypropylene fiber-reinforced concrete[J]. Sustainability Trends and Challenges in Civil Engineering: Select Proceedings of CTCS 2020, 2021: 799-812.

[7] Liang N, Geng S, Mao J, et al. Investigation on cracking resistance mechanism of basalt-polypropylene fiber reinforced concrete based on SEM test[J]. Construction and Building Materials, 2024, 411: 134102.

[8] Fredlund D, Xing A, Fredlund M, et al. The relationship of the unsaturated soil shear strength to the soil-water characteristic curve[J]. Canadian Geotechnical Journal, 1996, 33: 440–448.

[9] Acosta-Calderon S, Gordillo-Silva P, García-Troncoso N, et al. Comparative evaluation of sisal and polypropylene fiber reinforced concrete properties[J]. Fibers, 2022, 10(4): 31.

[10] Zhang X, Yin R, Chen Y, et al. Experimental study on the axial tensile properties of polypropylene fiber reinforced concrete[J]. Scientific Reports, 2023, 13(1): 16383.

[11] Blazy J, Blazy R. Polypropylene fiber reinforced concrete and its application in creating architectural forms of public spaces[J]. Case Studies in Construction Materials, 2021, 14: 00549.

[12] Zhou W, Mo J, Xiang S, et al. Impact of elevated temperatures on the mechanical properties and microstructure of waste rubber powder modified polypropylene fiber reinforced concrete[J]. Construction and Building Materials,2023, 392: 131982.

[13] Afroughsabet V, Ozbakkaloglu T. Mechanical and durability properties of high-strength concrete containing steel and polypropylene fibers[J]. Construction and Building Materials, 2015, 94: 73-82.

[14] Cui K, Xu L, Li X, et al. Fatigue life analysis of polypropylene fiber reinforced concrete under axial constant-amplitude cyclic compression[J]. Journal of Cleaner Production, 2021, 319: 128610.

[15] Hossain F, Pal A, Ahmed K, et al. Shear behavior of polypropylene fiber-reinforced concrete beams containing recycled aggregate and crumb rubber[J]. Journal of Cleaner Production, 2023, 412: 137370.

[16] Zhou M, He X, Wang H, et al. Mesoscale modeling of polypropylene fiber reinforced concrete under split tension using discrete element method[J]. Construction and Building Materials, 2023, 404: 133274.

[17] Zhou W, Mo J, Zeng L, et al. Fracture behavior of polypropylene fiber reinforced concrete modified by rubber powder exposed to elevated temperatures[J]. Construction and Building Materials, 2022, 346: 128439.

[18] Qin Y, Duan M, Ma W, et al. Experimental study on the damage permeability of polypropylene fiber-reinforced concrete[J]. Construction and Building Materials, 2021, 286: 122592.

[19] Lei L, Dong L, An H, et al. Experimental study of the thermal and dynamic behaviors of polypropylene fiber-reinforced concrete[J]. Applied sciences, 2021, 11(22): 10757.
[20] Wang C, Guo J, Li F, et al. Characterization of failure modes and mechanical behavior of micro-fiber-reinforced recycled aggregate concrete under Hopkinson pressure bar and in-situ CT techniques[J]. Construction and Building Materials, 2025, 458: 139726.
[21] Yan S, Dong Q, Chen X, et al. An experimental and numerical study on the hybrid effect of basalt fiber and polypropylene fiber on the impact toughness of fiber reinforced concrete[J]. Construction and Building Materials, 2024, 411: 134270.
[22] Ganorkar K, Goel M, Chakraborty T. Specimen size effect and dynamic increase factor for basalt fiber reinforced concrete using split Hopkinson pressure bar[J]. Journal of Materials in Civil Engineering, 2021, 33(12): 04021364.

Funding: This work was supported by the China Jiangxi Natural Science Foundation General Project (20232BAB204074).
[1]**First author resume:** Wang Youshi (1994 -), male, Shandong, PhD, Lecturer, Geotechnical Engineering, E-mail: wangyoushi1994@163.com.
***Corresponding author:** Lin Chao (1977 -), male, Shandong, PhD, professor, subterranean work, E-mail: 190125@jxycu.edu.cn.